Research Article | Vol. 7, No. 10 | 1 Oct 2017 | OPTICAL MATERIALS EXPRESS 3548
Optical Materials EXPRESS

Bismuth-doped hafnia-yttria-alumina-silica based fiber: spectral characterization in NIR to mid-IR

A. V. KIR'YANOV,[1,2,4] S. H. SIDDIKI,[2] Y. O. BARMENKOV,[1] D. DUTTA,[3] A. DHAR,[3] S. DAS,[3] AND M. C. PAUL[3,5]

[1]*Centro de Investigaciones en Optica, Loma del Bosque 115, Col. Lomas del Campestre, Leon 37150, Mexico*
[2]*National University of Science and Technology (MISIS), Leninsky Avenue 4, Moscow 119049, Russia*
[3]*Fiber Optics and Photonic Division, Central Glass & Ceramic Research Institute-CSIR, 196, Raja S.C. Mullick Road, Kolkata-700 032, India*
[3]*National University of Science and Technology (MISIS), Leninsky Avenue 4, Moscow 119049, Russia*
[4]*kiryanov@cio.mx*
[5]*paulmukul@hotmail.com*

Abstract: We report an experimental analysis of new hafnia-yttria-alumina-silica glass based fiber doped with bismuth (Bi), with absorption/fluorescence spectra along with resonant-absorption saturation, fluorescence lifetime, and gain, all adherent to Bi-related active centers (BACs), being measured at laser-diode excitation @ 908, 976, 1069, and 1120 nm, matching the NIR BACs' band. The found spectral laws reveal the optimal on excitation wavelength fluorescence, resonant-absorption bleaching, and gain capacities of the fiber, useful for applications at diode pumping. Besides, we report, for the first time to the best of our knowledge, a new resonant-absorption band of BACs in mid-IR (~2.1 μm) in the fiber, effectively bleached under the action of low-power in-band excitation, and provide the reasons for its association with co-doping the fiber with hafnium.

OCIS codes: (060.2290) Fiber materials; (160.2750) Glass and other amorphous materials.

References and links

1. V. V. Dvoyrin, V. M. Mashinsky, E. M. Dianov, A. A. Umnikov, and A. N. Guryanov, "Absorption, fluorescence and optical amplification in MCVD bismuth-doped silica glass optical fibers," in *Proc. 31st European Conference on Optics Communications* (Glasgow, Scotland, 2005) Paper Th.3.3.5, pp. 949–950.
2. E. M. Dianov, V. V. Dvoyrin, V. M. Mashinsky, A. A. Umnikov, M. V. Yashkov, and A. N. Guryanov, "CW bismuth fibre laser," Quantum Electron. **35**(12), 1083–1084 (2005).
3. I. Razdobreev, L. Bigot, V. Pureur, A. Favre, G. Bouwmans, and M. Douay, "Efficient all-fiber bismuth-doped laser," Appl. Phys. Lett. **90**(3), 031103 (2007).
4. E. M. Dianov, "Bi-doped optical fibers: a new active medium for NIR lasers and amplifiers," Proc. SPIE **6890**, 6890H (2008).
5. M. P. Kalita, S. Yoo, and J. Sahu, "Bismuth doped fiber laser and study of unsaturable loss and pump induced absorption in laser performance," Opt. Express **16**(25), 21032–21038 (2008).
6. V. G. Truong, L. Bigot, A. Lerouge, M. Douay, and I. Razdobreev, "Study of thermal stability and luminescence quenching properties of bismuth-doped silicate glasses for fiber laser applications," Appl. Phys. Lett. **92**(4), 041908 (2008).
7. V. V. Dvoyrin, V. M. Mashinsky, and E. M. Dianov, "Efficient bismuth-doped fiber lasers," IEEE J. Quantum Electron. **44**(9), 834–840 (2008).
8. I. A. Bufetov and E. M. Dianov, "Bi-doped fiber lasers," Laser Phys. Lett. **6**(7), 487–504 (2009).
9. V. V. Dvoyrin, A. V. Kir'yanov, V. M. Mashinsky, O. I. Medvedkov, A. A. Umnikov, A. N. Guryanov, and E. M. Dianov, "Absorption, gain and laser action in bismuth-doped aluminosilicate optical fibers," IEEE J. Quantum Electron. **46**(2), 182–190 (2010).
10. E. Dianov, "Bismuth-doped optical fibers: a challenging active medium for near-IR lasers and optical amplifiers," Light Sci. Appl. **1**(5), e12 (2012).
11. E. M. Dianov, S. V. Firstov, S. V. Alyshev, K. E. Riumkin, A. V. Shubin, V. F. Khopin, A. N. Gur'yanov, O. I. Medvedkov, and M. A. Mel'kumov, "A new bismuth-doped fibre laser, emitting in the range 1625–1775 nm," Quantum Electron. **44**(6), 503–504 (2014).

#302987 https://doi.org/10.1364/OME.7.003548
Journal © 2017 Received 21 Jul 2017; revised 21 Aug 2017; accepted 22 Aug 2017; published 12 Sep 2017

Optical Materials EXPRESS

12. I. A. Bufetov, M. A. Melkumov, S. V. Firstov, K. E. Riumkin, A. V. Shubin, V. F. Khopin, A. N. Guryanov, and E. M. Dianov, "Bi-doped optical fibers and fiber lasers," IEEE J. Sel. Top. Quantum Electron. **20**(5), 0903815 (2014).
13. Y. Fujimoto and M. Nakatsuka, "Infrared luminescence from Bismuth-doped silica glass," Jpn. J. Appl. Phys. 40(Part 2, No. 3B), L279–L281 (2001).
14. L. I. Bulatov, V. M. Mashinsky, V. V. Dvorin, E. F. Kustov, E. M. Dianov, and A. P. Sukhorukov, ""Structure of absorption and luminescence bands in aluminosilicate optical fibers doped with bismuth," Bull. Russ. Acad," Sci. **72**, 1655–1660 (2008).
15. M. A. Hughes, T. Suzuki, and Y. Ohishi, "Compositional optimization of bismuth-doped yttria–alumina–silica glass," Opt. Mater. **32**(2), 368–373 (2009).
16. M. Peng, C. Zollfrank, and L. Wondraczek, "Origin of broad NIR photoluminescence in bismuthate glass and Bi-doped glasses at room temperature," J. Phys. Condens. Matter **21**(28), 285106 (2009).
17. S. Khonton, S. Morimoto, Y. Arai, and Y. Ohishi, "Redox equilibrium and NIR luminescence of Bi_2O_3–containing glasses," Opt. Mater. **31**(8), 1262–1268 (2009).
18. V. O. Sokolov, V. G. Plotnichenko, V. V. Koltashev, and E. M. Dianov, "Centres of broadband near-IR luminescence in bismuth-doped glasses," J. Phys. D Appl. Phys. **42**(9), 095410 (2009).
19. Y. Fujimoto, "Local structure of the infrared bismuth luminescent center in Bismuth-doped silica glass," J. Am. Ceram. Soc. **93**(2), 581–589 (2010).
20. I. Razdobreev, H. El Hamzaoui, L. Bigot, V. Arion, G. Bouwmans, A. Le Rouge, and M. Bouazaoui, "Optical properties of Bismuth-doped silica core photonic crystal fiber," Opt. Express **18**(19), 19479–19484 (2010).
21. A. V. Kir'yanov, V. V. Dvoyrin, V. M. Mashinsky, Y. O. Barmenkov, and E. M. Dianov, "Nonsaturable absorption in alumino-silicate bismuth-doped fibers," J. Appl. Phys. **109**(2), 023113 (2011).
22. A. V. Kir'yanov, V. V. Dvoyrin, V. M. Mashinsky, N. N. Il'ichev, N. S. Kozlova, and E. M. Dianov, "Influence of electron irradiation on optical properties of Bismuth doped silica fibers," Opt. Express **19**(7), 6599–6608 (2011).
23. S. V. Firstov, V. F. Khopin, I. A. Bufetov, E. G. Firstova, A. N. Guryanov, and E. M. Dianov, "Combined excitation-emission spectroscopy of bismuth active centers in optical fibers," Opt. Express **19**(20), 19551–19561 (2011).
24. V. O. Sokolov, V. G. Plotnichenko, and E. M. Dianov, "Interstitial BiO molecule as a broadband IR luminescence centre in bismuth-doped silica glass," Quantum Electron. **41**(12), 1080–1082 (2011).
25. M. Peng, G. Dong, L. Wondraczek, L. Zhang, N. Zhang, and J. Qiu, "Discussion on the origin of NIR emission from Bi-doped materials," J. Non-Cryst. Solids **357**(11-13), 2241–2245 (2011).
26. B. Xu, S. Zhou, M. Guan, D. Tan, Y. Teng, J. Zhou, Z. Ma, Z. Hong, and J. Qiu, "Unusual luminescence quenching and reviving behavior of Bi-doped germanate glasses," Opt. Express **19**(23), 23436–23443 (2011).
27. D. A. Dvoretskii, I. A. Bufetov, V. V. Vel'miskin, A. S. Zlenko, V. F. Khopin, S. L. Semjonov, A. N. Gur'yanov, L. K. Denisov, and E. M. Dianov, "Optical properties of bismuth-doped silica fibers in the temperature range 300-1500 K," Quantum Electron. **42**(9), 762–769 (2012).
28. V. O. Sokolov, V. G. Plotnichenko, and E. M. Dianov, "Origin of near-IR luminescence in Bi_2O_3-GeO_2 and Bi_2O_3-SiO_2 glasses: first-principle study," Opt. Mater. Express **5**(1), 163–168 (2015).
29. K. E. Riumkin, M. A. Melkumov, I. A. Varfolomeev, A. V. Shubin, I. A. Bufetov, S. V. Firstov, V. F. Khopin, A. A. Umnikov, A. N. Guryanov, and E. M. Dianov, "Excited-state absorption in various bismuth-doped fibers," Opt. Lett. **39**(8), 2503–2506 (2014).
30. D. Ramirez-Granados, Y. Barmenkov, A. Kir'yanov, V. Aboites, M. Paul, A. Halder, S. Das, A. Dhar, and S. Bhadra, "The use of yttria-alumino-silicate bismuth doped fibers for temperature sensing," IEEE Photonics J. **7**(4), 6802112 (2015).
31. A. V. Kir'yanov, A. Halder, Y. O. Barmenkov, S. Das, A. Dhar, S. K. Bhadra, V. G. Plotnichenko, V. V. Koltashev, and M. C. Paul, "Distribution of bismuth and bismuth-related centers in core area of Y-Al-SiO_2:Bi fibers," IEEE J. Lightw. Technol. **33**(17), 3649–3659 (2015).
32. M. Dult, R. S. Kundu, N. Berwal, R. Punia, and N. Kishore, "Manganese modified structural and optical properties of bismuth silicate glasses," J. Mol. Struct. **1089**, 32–37 (2015).
33. E. M. Dianov, "Nature of Bi-related near IR active centers in glasses: state of the art and first reliable results," Laser Phys. Lett. **12**(9), 095106 (2015).
34. Y. Zhao, L. Wondraczek, A. Mermet, M. Peng, Q. Zhang, and J. Qiu, "Homogeneity of bismuth-distribution in bismuth-doped alkali germanate laser glasses towards superbroad fiber amplifiers," Opt. Express **23**(9), 12423–12433 (2015).
35. D. L. Wood, K. Nassau, T. Y. Kometani, and D. L. Nash, "Optical properties of cubic hafnia stabilized with yttria," Appl. Opt. **29**(4), 604–607 (1990).
36. D. Neumayer and E. Cartier, "Materials characterization of ZrO_2-SiO_2 and HfO_2-SiO_2 binary oxides deposited by chemical solution deposition," J. Appl. Phys. **90**(4), 1801–1808 (2001).
37. S. Todoroki, K. Hirao, and N. Soga, "Origin of inhomogeneous linewidth of Eu^{3+} fluorescence in several oxide glasses," J. Appl. Phys. **72**(12), 5853–5860 (1992).
38. A. V. Kir'yanov, S. H. Siddiki, Y. O. Barmenkov, S. Das, D. Dutta, A. Dhar, V. G. Plotnichenko, V. V. Koltashev, A. V. Khakhalin, E. M. Sholokhov, N. N. Il'ichev, S. I. Didenko, and M. C. Paul, "Hafnia-yttria-alumina-silicate optical fibers with diminished mid-IR (>2 μm) loss," Opt. Mater. Express **7**(7), 2511–2518 (2017).

Optical Materials EXPRESS

39. D. Benerjee, P. Das, R. Guin, and S. K. Das, "Nuclear quadrupole interaction at ^{181}Ta in hafnium dioxide fiber: Time differential perturbed angular correlation measurements and ab-initio calculations," J. Phys. Chem. Solids **73**(9), 1090–1094 (2012).
40. D. Ramirez-Granados, A. V. Kir'yanov, Y. O. Barmenkov, A. Halder, S. Das, A. Dhar, M. C. Paul, S. Bhadra, S. I. Didenko, V. V. Koltashev, and V. G. Plotnichenko, "Effects of elevating temperature and hightemperature annealing upon state-of-the-art of yttia-alumino-silicate fibers doped with Bismuth," Opt. Mater. Express **6**(2), 486–508 (2016).
41. J. Lee, M. Jung, M. Melkumov, V. F. Khopin, E. M. Dianov, and J. H. Lee, "A saturable absorber based on bismuth-doped germanosilicate fiber for a 1.93 μm, mode-locked fiber laser," Laser Phys. Lett. **14**(6), 065104 (2017).

1. Introduction

Interest to Bismuth (Bi) doped silica fibers (hereafter – BDFs) is now increasing given that they exhibit remarkably broadband near-infrared (NIR) fluorescence and gain, spanning a ~1.1 to 1.8 μm region when pumped at ~450 nm to ~1.5 μm. Since invention of the first BDF based laser [1,2], a line of compact and easy in assembling fiber lasers and amplifiers employing BDFs have been reported; see e.g [3–12]. Depending on core-glass composition, Bi-related active centers (further – BACs) of different types, fluorescing in the visible (VIS) to NIR, can be produced [13–34]; in majority of cases, such centers are capable of amplifying and lase. Particularly, strong fluorescent ability of BACs formed in aluminosilicate (AS) glass and fiber, associated with the presence of Aluminum (Al), was shown to result in low-threshold (units of W) lasing at wavelengths covering the ~1.15…~1.25-μm range when pumped at ~1.0…~1.1 μm. Special interest to AS BDFs stems from the fact that pump wavelengths at which BACs of this type are excited coincide with the operation ones of 'conventional' high-power Ytterbium fiber lasers. It is also worth noticing that the spectral range of amplifying/lasing (~1.15…~1.25 μm), accessible with AS BDFs, matches well the one where fundamental loss of silica fiber is minimal, which is indispensable for next-day telecom needs. On the other hand, the nature of BACs responsible for the broadband NIR fluorescence of BDFs, including the ones with AS core-glass, is yet disputing; moreover, opinions about a type of such BACs (hereafter we specify them Bi(Al)) are controversial. Thus, it is not surprising that the unfavorable situation with uncertain nature of Bi(Al) BACs, formed in fiber of this type, and, eventually, misunderstanding of their functionality at excitation into their absorption bands limit progress in the area. Among hard of solving other problems, one is limited efficiency of lasing at ~1.15…1.25 μm using AS BDFs (it never exceeds 30%), as compared with BDFs with phosphosilicate, germanosilicate, or purely silicate core. As has been recently shown, one of probable reasons behind this disadvantage are Bi concentration effects, viz. BACs clustering, leading to up-conversion (UC) of homogeneous and inhomogeneous type [5,9,26,29,31,33].

In the current study, we report the fabrication of a new kind of AS BDF, the hafnia (Hf) and yttria (Y) co-doped aluminosilicate (HYAS) BDF, and comprehensively analyze its spectral properties. Our experimental analysis comprises the measurements of absorption and fluorescence spectra of the fiber along with resonant-absorption bleaching, NIR fluorescence lifetime, and gain, obtained at excitation at different wavelengths in NIR (908, 976, 1064, and 1120 nm), all falling into the ~1-μm absorption band of Bi(Al) BACs. We also present the data for this fiber, revealing the presence of a resonant-absorption band of BACs in mid-IR (at ~2.05 μm), never reported for AS-BDFs, and its bleaching at 'in-band' low-power excitation. These are compared with the ones obtained with 'standard' (Hf/Y free) BDFs. Note that the HYAS-BDF is a new material, though BDFs with Hf-free core-glass have been reported earlier [30,31].

Our motivation to fabricate a BDF with HYAS core-glass had the following bases. Fibers of such type are expected to have reduced, as compared to standard silica-based ones, effective phonon energy and, hence, reduced fundamental loss in mid-IR. The idea to develop such BDF also stems from the known fact that HfO_2 is a material with a high refractive index (RI), transparent over a wide spectral range, ~0.4 to ~6 μm [35]. We have chosen this kind of

Optical Materials EXPRESS

core-glass as promising for high-power laser applications, requiring a high optical-damage threshold (HfO_2 belongs to this class of oxides). Also, note that in silicates Hf ions are coordinated to more than four oxygen atoms, with creation of non-bridging oxygens (NBOs) in silica network [36]. Flexibility of such network seems to be high (given the presence of NBOs), thus, allowing the host glass to accommodate, in almost equivalent environments, optically-active co-dopants, e.g. rare-earths or post-transitional metals such as Bi [37]. Then, we considered HfO_2 as capable to modify the overall core-glass structure and, thus, facilitate the dispersion of 'active' co-dopants (in our case, Bi) and, eventually, diminish clustering of BACs and related deteriorating UC-phenomena. Besides, the presence of Hf ions in core-glass of AS type may affect the local structure of Bi(Al) BACs and/or be responsible for formation in HYAS-BDF of BACs of other type, associated with the Hf-subsystem. Thus, it was interesting to check the both guesses. As shown at the end of this study, co-doping of AS-BDF with Hf does result in creating of optically active Bi,Hf-related centers with a 'spectral signature' in mid-IR (near and beyond 2 μm).

2. Material properties and experimental techniques

2.1. Fabricating and basic properties

The HYAS-DBF has been fabricated using a standard drawing tower from a nano-engineered HYAS-based preform, obtained through the Modified Chemical Vapor Deposition (MCVD) process gathered with the solution-doping (SD) technique, then followed by suitable thermal treatment. The glass modifiers (Al_2O_3, Y_2O_3, HfO_2, and Bi_2O_3) were incorporated via SD; soaking of porous soot layers of the sourcing tube was done into solution of alcoholic-water (1:5) mixture ($Al(NO_3)_3$: $9H_2O$, YCl_3: $6H_2O$, $HfOCl_3$: $8H_2O$, and $Bi(NO_3)_3$: H_2O) during ~1 h. After draining out the solution, the core layer was dried with flow of N_2 gas at room temperature and dried thermally, by heating up to ~500°C with flow of mixture of O_2 and He gases, for oxidizing the salts. Sintering of the layers and collapsing of the tube were proceeding in atmosphere of the same gases at higher temperatures, 1800°C and 2200°C, respectively. The preform was then thermally annealed at ~1000°C in a controlled heating furnace, which gave rise to creating Bi-doped HYAS core-glass of ceramic type. This preform was finally over-cladded to get, after drawing, a single-mode fiber. For drawing the fiber (at ~2000°C), we used a conventional fiber drawing tower. The final over-cladded HYAS-BDF has 125.0/2.9-μm clad/core diameters and numerical aperture (NA) of 0.24. Note that its version without over-cladding with 125.0/11.1-μm clad/core diameters has been studied in [38].

Doping the preform with Al_2O_3 had the following justifications: apart of Al being a pre-requisite for creating Bi(Al) BACs, its addition permits engineering of fiber's NA and enhances chemical durability of core-glass. In turn, doping with Y_2O_3 solves the tasks of facilitating the radiative transitions between the electronic levels of BACs (phonon energy of Y_2O_3 is one of the lowest cutoffs among oxides) and, eventually, enhancing the fluorescent ability of BACs. The role of co-doping with HfO_2 was addressed above; see Section 1.

Doping levels of the core-glass formers (Al_2O_3, Y_2O_3, HfO_2, and Bi_2O_3) were measured with multimode version of HYAS-BDF with a bigger (~11 μm) core, employing Electron Probe Micro Analysis (EPMA). The radial distributions of co-dopants are shown in Fig. 1(a). In turn, radial distribution of the fiber's RI (Fig. 1(b)) was measured using a fibered RI-profilometer. As seen from Fig. 1(a), we were successful in co-doping the fiber with Hf at SD: HfO_2 content reached ~1 mol.% (see the orange curve in the figure). Bi has been embedded in the amount we targeted (~0.25 mol.% of Bi_2O_3: see the grey curve, zoomed in the inset to Fig. 1(a)). Note that weak doping with Bi was chosen to avoid, or at least, minimize, BACs' clustering. The radial distributions of Al_2O_3 and Y_2O_3 are demonstrated in Fig. 1(a) by black and magenta curves, respectively (for Y_2O_3, it is zoomed in the inset for comparing with that for Bi_2O_3). Molar percentages of all oxides forming the fiber's core-glass were roughly proportional to the correspondent salts' contents, soaked into the preform at SD.

Optical Materials EXPRESS

On the other hand, surprisingly, the HYAS-BDFs, obtained with and without high-temperature over-cladding, demonstrate quite different extinctions in BACs' bands: the over-cladded HYAS-BDF (under scope as follows) has much more intensive absorptions in all the bands. This fact deserves a separate study; here we only fix the point while note that, given by the results of our previous work on impact of high temperature on properties of AS BDFs without Hf co-doping [30,40], the high-temperature annealing (at ~2000°C), inherent to the process of over-cladding, can be an explanation of the phenomenon because Bi_2O_3 is strongly volatilizing upon heating.

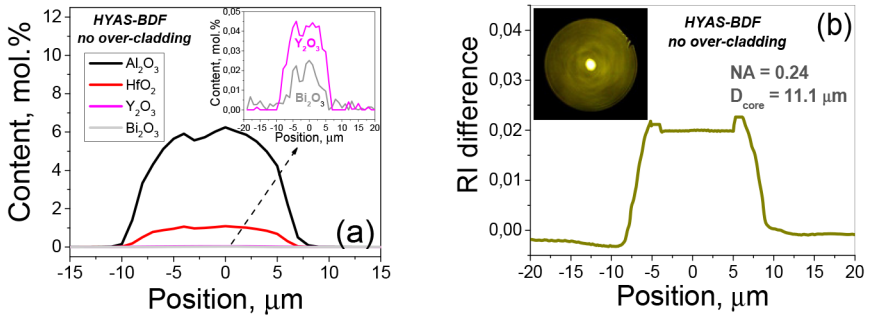

Fig. 1. (a) Radial distributions of the oxides constituting core-glass of multimode HYAS-BDF (without over-cladding), Al_2O_3, HfO_2, Y_2O_3, and Bi_2O_3, obtained from the EPMA analysis, in mol.%; for Bi_2O_3 and Y_2O_3, the distributions are zoomed in inset. (b) Radial distribution of RI-difference, measured before over-cladding; inset: image of cleaved fiber.

Then, as seen from Fig. 1(b), big RI-difference between core and cladding reveals a considerable effect of Hf co-doping (though Hf-content in the fiber's core-glass is low – refer to Fig. 1(a)) on refractive and, hence, wave-guiding, properties of the fiber, but it is an expected result as HfO_2 is a highly refractory oxide (see e.g [39].).

2.2. Experimental equipment and techniques

For spectral measurements, three optical spectrum analyzers (OSAs) were employed: *Ando* AQ6315A (OSA1), *Yokogawa* AQ6375 (OSA2), and *Thorlabs* 203 (OSA3), with optical bands 400…1650 nm, 1200…2400 nm, and 1000…2500 nm, respectively. To pump the fiber into the NIR band (~1 μm), associated with the presence of Bi(Al) BACs, we experimented with a set of laser diodes (LDs) with fiber outputs, operating at: λ_{P1} = 908 nm, λ_{P2} = 976 nm, λ_{P3} = 1069 nm, and λ_{P4} = 1120 nm; LDs were from *Q-Photonics* (the first three) and *Innolume* (the last one). The LDs' single-mode output fibers were easily and almost lossless spliced with the HYAS-BDF. In addition, to excite the HYAS-BDF in mid-IR, we handled a superfluorescent broadband 2-μm source (central wavelength, λ_{P5} = 2.07 μm) with 11-mW output; in this case, output light was coupled into the fiber through a single-mode patch-cord and fiber adapter.

To measure attenuation spectra (see Fig. 2 and Fig. 10), we used a white-light (WL) fiber-adapted source (*Yokogawa* AQ4305). The BDF's optical transmission spectra were measured by the cutback method. Fiber samples were WL-illuminated and the measured transmission spectra were then re-calculated into the spectra of 'small-signal' absorption $\alpha_0(\lambda)$ (in dB/m).

Fluorescence spectra of the HYAS-BDF in NIR (see Fig. 3 and Fig. 9) were measured either in 'forward' or 'backward' geometry, at excitation at LDs' wavelengths λ_{P1}…λ_{P4}. In the first case, NIR fluorescence and rest of pump light were directly delivered to OSA1/OSA2. In the second case, a 2 × 1 fused fiber wavelength-division multiplexer (WDM) was used to assemble backward geometry. One of the WDM's input ports was spliced to a LD's output pigtail, whereas its output port – to a HYAS-BDF sample; the other input port was connected to OSA, thus permitting capture of fluorescence propagating backward. Backward geometry

Optical Materials EXPRESS

is impossible at the use of forward geometry, i.e. without filtering. For measurements in mid-IR, given that >2-μm emission at excitation at λ_{P5} was weak, we employed forward geometry and OSA3 for displaying the spectra: OSA of this type permits this in 'endless' acquitting mode.

The HYAS-BDF's gain (G) spectra in NIR (see Fig. 5), were obtained applying the following procedure. A HYAS-BDF sample was pumped from its one side by a LD through the same WDM while WL was launched from its opposite side. By means of measuring the fiber's fluorescence spectra at WL switched ON and OFF, then measuring its attenuation spectrum without pumping (but with WL switched ON), and posterior data processing, normalized gain spectra (G/α_0) were found.

At fluorescence lifetime measurements (see Fig. 4), a NIR (up to 1.6 μm) fluorescence signal from a HYAS-BDF sample was captured at fast switching pump-light OFF (before blocking, pump power was fixed at maximum). To diminish pump background in the measured signal, a long-pass optical filter with ~1000-nm cut-on (*Thorlabs* FEL1000) was placed between the sample and a Ge photo-detector (*Newport* 2033, 200-kHz bandwidth). The time resolution of the measurements was ~1.5 μs.

We also studied nonlinear absorption of the HYAS-BDF at all pump wavelengths (i.e. at $\lambda_{P1}\ldots\lambda_{P5}$) in function of pump power P_{in}; see Figs. 6, 7, and 8. We found dependences of nonlinear-absorption coefficient $K_{NL}(P_{in})$ as follows. Pump light from a LD was launched through splice to a HYAS-BDF sample of length L_f. First, we measured (with a power-meter *Thorlabs*) its nonlinear transmission: $T_{NL} = P_{out}/P_{in}$ (P_{out} is a part of pump power, residing at the sample's output) and then made formal re-calculation of T_{NL} in nonlinear absorption via relationship: $K_{NL}(P_{in}) = -\ln(T_{NL})/L_f$.

3. Experimental results and discussion

3.1. Spectral characteristics in near-IR (~1-μm region)

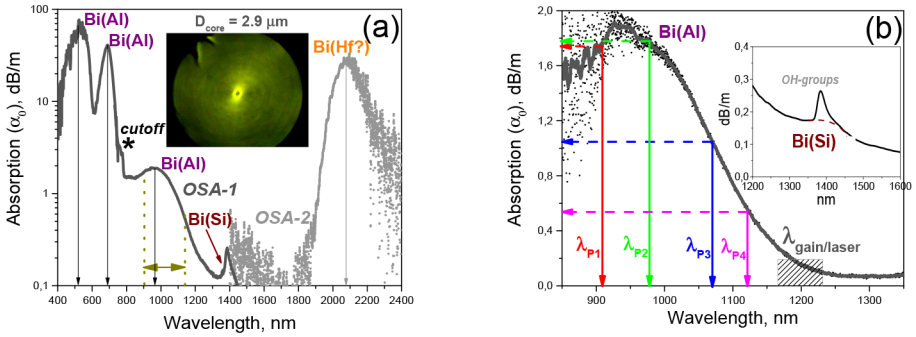

Fig. 2. Absorption spectra of HYAS-BDF: (a) in the whole spectral range spanned (using OSAs 1 & 2), where are specified the absorption peaks related to BACs Bi(Al) and cutoff peak (inset demonstrates the cross-sectional image of the fiber); (b) the ~1-μm BACs absorption band (enlarged), where are shown (by different colors) the pump wavelengths (908, 976, 1069, and 1120 nm), used in experiments (inset demonstrates the spectral region where the losses produced by OH-overtones and by BACs Bi(Si) are superimposed). λ_{Pi} and $\lambda_{gain/laser}$ define the spectral positions of the four pump and potential gain/laser wavelengths.

As known, BACs in AS BDFs are defined by three resonant-absorption bands, centered at ~500, ~700, and ~1000 nm, all adherent to BACs of Bi(Al) type, and by the band at ~1.4 μm (characteristic to BACs, associated with Silicon, Bi(Si); the last one is usually overlapped with the absorption line of hydroxyl groups (at ~1.38 μm). As seen from Fig. 2, where we provide the absorption spectrum of the HYAS-BDF, all these bands, located in VIS to NIR,

Optical Materials EXPRESS

are present in our fiber as it certainly is a kind of AS BDFs with addition of Hf and Y: refer to Fig. 1(a). In Fig. 2(a), we designate them accordingly: Bi(Al) and Bi(Si).

Furthermore, the HYAS-BDF demonstrates an intensive absorption band in mid-IR, at ~2.05…2.1 μm. Note that such spectral feature was never reported for 'conventional' (Hf/Y-free) AS BDFs. In our opinion, it deserves attention and will be studied in more detail below, in subsection 3.2. Also, note that the HYAS-BDF has in mid-IR but off this band (i.e. at λ~2.4 μm), lower fundamental loss than it is characteristic for Hf-free silica fibers. This advantage, already reported, has been established to originate from co-doping with HfO_2 [38].

In Fig. 2(b), we zoom the NIR Bi(Al) band at ~1.0 μm where by arrows of different colors are shown the pump wavelengths $\lambda_{P1}…\lambda_{P4}$, chosen to study fluorescence/gain capabilities of the fiber in NIR. We also highlight in Fig. 2(b) the wavelengths (see the dashed box), at which in AS BDFs is accessible gain/lasing. Besides, we provide in inset to Fig. 2(a) the image of a cleaved HYAS-BDF sample, revealing reduced after over-cladding core (~3.0 μm) and single-mode guidance at λ>800 nm (compare with the image of its multimode analog in Fig. 1(b)).

In Fig. 3, we present the fluorescence spectra of the HYAS-BDF at NIR excitations, measured in (a) forward and (b) backward geometries, respectively. The first spectra, obtained at varying fiber length to provide equal optical density at each pump wavelength, allow one to reveal relative (vs. pump wavelength) fluorescence capabilities of the fiber. The second ones, for comparison, were obtained at handling the same fiber length (30 cm). In both circumstances, launched pump power was fixed to 150 mW, at each λ_{Pi}, for direct comparison of the results.

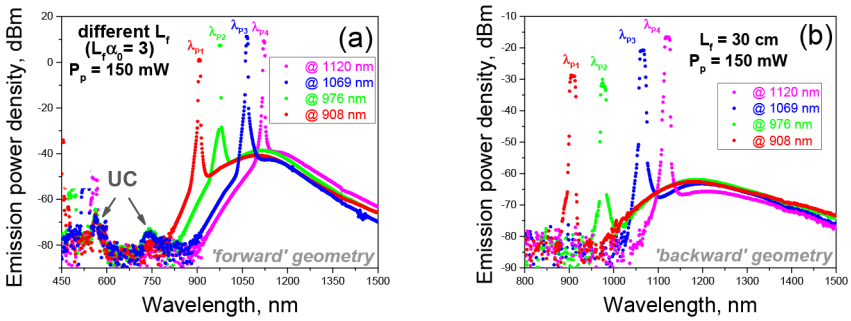

Fig. 3. Fluorescence spectra of HYAS-BDF, obtained in 'forward' (a) and 'backward' (b) geometries at excitation at 908, 976, 1069, and 1120 nm, shown by different colors. The spectra were measured at P_P = 150 mW, at either pump wavelength. The 800…1600 nm fluorescence is inherent to Bi(Al) BACs.

Note here that NIR fluorescence, ranging from 800 to 1600 nm, is characteristic for Bi(Al) BACs. As seen from Fig. 3, the NIR fluorescence spectra are quite similar at λ>1.15 μm, while if a pump wavelength is shortened the fluorescence spectrum gets broaden, spanning to anti-Stokes side. It is also seen from the figure that UC emissions in VIS are very weak in intensity. Weakness of UC emissions reveals insignificant excited-state absorption (ESA) at any pump wavelength falling in the ~l-μm absorption band and, also, insignificant concentration effects via BACs clustering. Then, as stems from comparison of panels (a) and (b) in Fig. 3, excitation at a longer wavelength (especially, at 1120 nm) looks more favorable for amplifying/lasing despite optical density of the fiber at such wavelengths is smaller (α_0 is measured by ~0.5 dB/m @1120 nm, ~1.0 dB/m @1069 nm, and ~1.8 dB/m @908 / @967 nm: refer to (Fig. 2(b)).

The Bi(Al) related NIR (>1 μm) fluorescence lifetimes at different pump wavelengths were measured in backward geometry for diminishing the role of spectrally different optical

Optical Materials EXPRESS

density. The data for lifetimes obtained for all pump wavelengths are plotted in main frame of Fig. 4 and the examples of fluorescence kinetics at 150-mW pump are demonstrated in inset.

It is seen from Fig. 4 that the NIR fluorescence lifetime is around 1.1 ms, exceeding the biggest values so-far reported for Hf-free AS BDFs (~0.9 ms; see e.g [9].); certainly, an increase of NIR fluorescence lifetime is an advantage of the HYAS-BDF. It deserves noticing that lifetime is independent of pump power, for all excitation wavelengths. Also note that (see inset) the fluorescence obeys a nearly exponential law of decaying at NIR excitation (only for λ_{P1} = 908 nm it gets slightly deviated from exponent). Thus, we can conclude about none or negligible deteriorating effects, such as UC and clustering of fluorescence-active Bi(Al) centers, in the HYAS-BDF. This favorably differs this type of fiber from Hf-free BDF analogs, for which it is known that, yet at much lower Bi(Al) BACs concentrations, NIR fluorescence decay strongly deviates from exponent because of concentration-related UC effects [9,21]. Longer NIR fluorescence lifetime in the HYAS-BDF can be explained by a favorable role of co-doping with HfO_2 – via facilitating dispersion and homogenization of BACs distribution in core-glass – in diminishing the BACs clustering and, eventually, weakening UC.

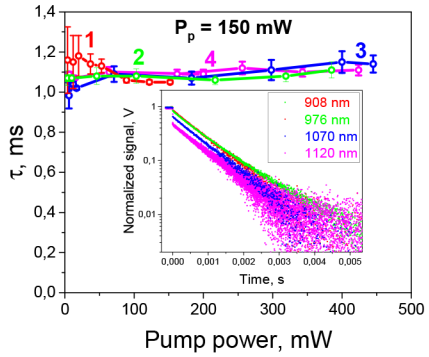

Fig. 4. NIR (1.1…1.5 μm) fluorescence decay in HYAS-BDF. (main frame) Fluorescence lifetime *vs.* pump power (at excitation @908, 976, 1069, and 1120 nm; see curves 1 to 4 of different colors). (inset) Dependences of fluorescence signals *vs.* time, for P_P = 150 mW.

We have also made insight to the spectral character of amplifying (gain) potential of the HYAS-BDF. Note that laser action with this fiber was hardly expectable given its large absorption coefficient in the ~1-μm band (~0.5…~1.8 dB/m at λ_{P4}…λ_{P1}; see Fig. 2) at pumping by weak-power LDs; indeed, our attempt to turn the HYAS-BDF to lase has failed. However, we can compare spectral character of the fiber's gain potential at pumping at λ_{Pi} (i = 1…4). In Fig. 5, we present the results obtained for normalized gain (G/α_0) at these excitations.

Optical Materials EXPRESS

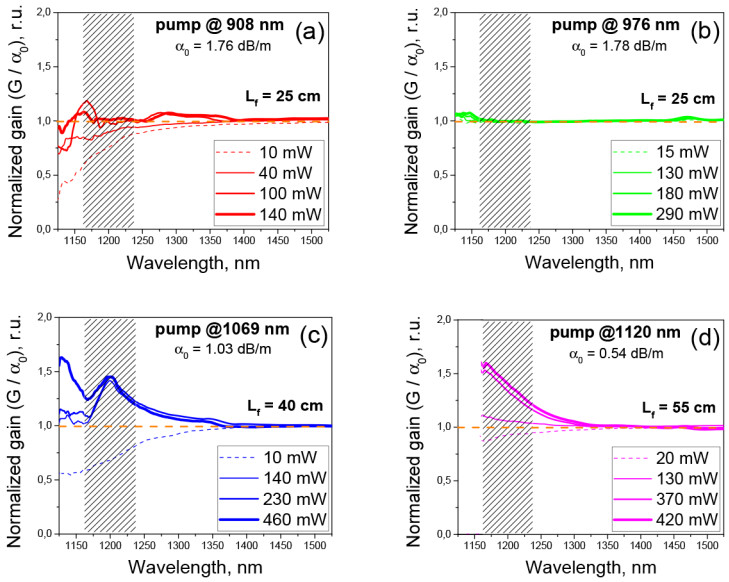

Fig. 5. Spectral dependences of on-off normalized (G/α_0) gain in HYAS-BDF, measured as functions of pump wavelengths: 908 (a), 976 (b), 1069 (c), and 1120 (d) nm). Each set of the dependences in (a-d) was obtained for a few pump powers, specified in insets. Lengths of HYAS-BDF L_f were chosen such that the product $L_f\alpha_0$ equals to 0.4…0.5, at each λ_{Pi}. Dashed orange line fits the eye to the level $G/\alpha_0 = 1$.

As seen from Fig. 5, gain in the HYAS-BDF is much greater at pumping @1069 and @1120 nm (for which maximal G/α_0-values, of ~1.5, are attainable in the 1.17…1.22-μm domain) than @908 and @976 nm (for which G/α_0 is either negative, or ~1). This situation reminds the known one that an optimal for amplifying/lasing pump wavelength is around 1.07 μm, not once confirmed for Hf-free AS BDFs. Possible reasons for poorer performance of the HYAS-BDF at pumping below ~1 μm can be ESA in the system of Bi(Al) BACs, resonant to excitation in this spectral range, or an absorption band below 1 μm, produced by other, non-Bi(Al), centers, hardly or not saturated under the action of resonant radiation.

In Fig. 6, we demonstrate the results revealing the spectral trends that nonlinear (viz. bleachable under the action of light) absorption K_{NL} of the HYAS-BDF obeys, at different pump wavelengths. (Note that below, in Fig. 7, we build the quantities, representing these trends in more explicit manner, found from the dependences of nonlinear-absorption vs. pump power.) Fiber lengths used in the experiments were chosen to be back-proportional to small-signal absorptions α_0 (asterisked in each panel (a-d)). This ensured that optical densities of the fiber samples under test were similar, likewise in the experiments on measuring NIR fluorescence and gain (see Figs. 3(a) and 5). Note that the horizontal dashed arrows in Fig. 6 mark the plateaus, to which absorption approaches at pumping at each wavelength.

Optical Materials EXPRESS

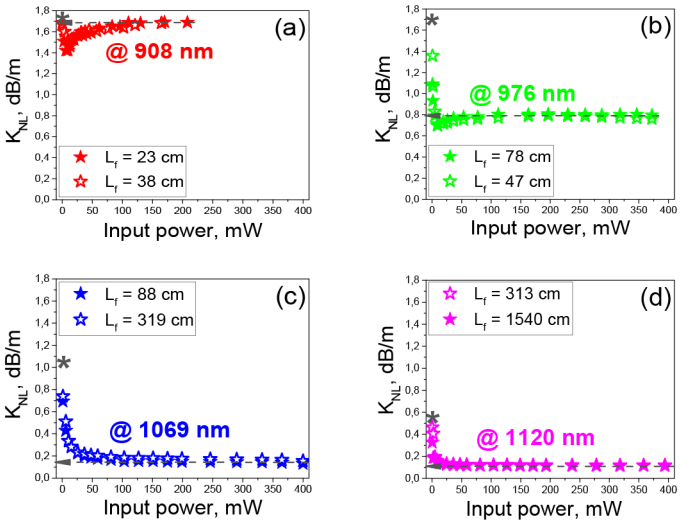

Fig. 6. Nonlinear absorption (K_{NL}) of HYAS-BDF: Dependences of K_{NL} measured in function of pump wavelengths (a-d), where black asterisks show the 'initial' (small-signal) absorptions at these wavelengths, obtained from the absorption spectra, using OSA1 (refer to Fig. 1). For each pump wavelength, the data obtained with two HYAS-BDF lengths L_f, (insets) are plotted. Dashed arrows show the levels of un-bleached absorptions.

As seen from Fig. 6, the dependences K_{NL} vs. P_{in} differ strongly for different λ_{pi}, that is, if pump wavelength is above 1 μm (1069 (c) and 1120 nm (d); see two lower panels in Fig. 6), absorption is easily bleachable yet at small launched powers (a few to ten mW, @1120 and @1069 nm, respectively). Remarkably, in these two cases, the HYAS-BDF is bleached down to ~0.1 and ~0.15 dB/m. In contrast, if pump wavelength is below 1 μm (976 (b) and 908 nm (a); see two upper panels in Fig. 6), absorption is bleached either partially (b) or is retrieved up to almost its initial level (a) (after 'sliding down' but slightly at small pumps). As seen from (b) and (a), the 'final' (at maximal pump), absorptions are measured by ~0.8 and ~1.7 dB/m: compare these values with 'small-signal' absorptions at these wavelengths (~1.8 dB/m).

Thus, the examination of the presented set of dependences turns us to conclude that, when pump light matches the right slope of the ~1-μm absorption band of Bi(Al) BACs (refer to Fig. 2(b)), the fiber is effectively bleached and has small residual absorption, measured by 0.1…0.15 dB/m; however, if pump light matches the central part or left slope of the band, it demonstrates only partial (on a level of ~55%) or almost none bleaching. As seen, the found spectral laws are in parallel to the ones found in our experiments on gain measurements: compare panels (a-d) in Figs. 6 and 5. Besides, the presence of big residual absorption under pumping (Fig. 6(a),6(b)) and, accordingly, small or negligible gain (Fig. 5(a). 5,(b)) may indicate the presence of ESA (spectrally dominating at shorter wavelengths in the ~1-μm absorption band of Bi(Al) BACs) or be a contribution stemming from other centers of yet uncovered nature.

In Fig. 7, we quantify the found trends in simpler but physically clearer terms. Namely, we show in the figure the spectral behaviors of the initial (small-signal, α_0) absorption, see orange curve 1 (in fact, copied from Fig. 2(b), obtained from the measurements using OSA), and unbleached (or residual, α_{res}) absorption, see violet curve 2 (in fact, K_{NL}-values, designated by dashed horizontal arrows in panels (a-d) of Fig. 6, to which nonlinear absorptions approach at maximal available pumps, at different wavelengths). As seen from comparison of curves 1 and 2, both absorptions steadily decrease with wavelength but obey different spectral laws, ~(1–exp(-P_{in})) and ~exp(-P_{in}), correspondingly. Then, subtracting

Optical Materials EXPRESS

spectrum 2 from spectrum 1 and normalizing the result, we find the 'bleaching contrast' of the HYAS-BDF (see spectrum 3 in Fig. 7(b)), having a 'parabolic' law of spectral changes. From the last dependence, we conclude that the most promising pump wavelength is ~1025 nm (see the dotted line), at which ground-state absorption of BACs Bi(Al) is mostly effective bleached. Around this wavelength the fiber becomes amplifying and (expectedly) capable of lase.

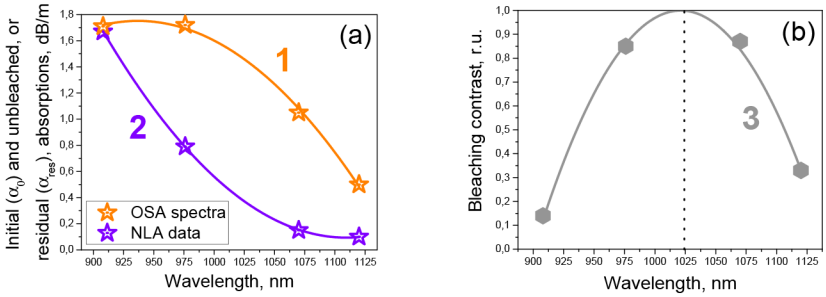

Fig. 7. (a) Spectral dependences of small-signal (curve 1) and un-bleached (curve 2) absorptions and (b) spectrum of 'bleaching contrast' (curve 3) of HYAS-BDF.

3.2. Spectral features in mid-IR (~2-μm region)

As demonstrated above, general appearance of the HYAS-BDF in the NIR is reminiscent of other, but Hf-free, AS BDFs. However, the presence of the absorption band in the mid-IR (peaking at ~2.05…2.1 μm: refer to Fig. 2(a)), which is assumingly related to co-doping the fiber with Hf/Y, requires separate insight. Below we make such insight that includes (i) an observation of the effect of this band's effective bleaching under the action of broadband 11-mW ~2.07-μm light (Fig. 8) and (ii) direct comparison of NIR/mid-IR attenuation spectra of the HYAS-BDF and those of a set of similar in composition but Hf/Y-free fibers (Fig. 9).

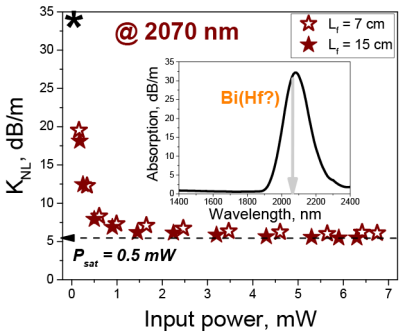

Fig. 8. (main frame) Nonlinear absorption K_{NL} of HYAS-BDF: Dependences of K_{NL} *vs.* pump power of broadband emission with central wavelength 2070 nm (black asterisk shows 'initial', or small-signal, absorption at this wavelength). The data were obtained using two fiber lengths (7 and 15 cm). Dashed arrow shows the level of un-saturated part of absorption (~15%). (inset) Absorption spectrum of HYAS-BDF in mid-IR at linear scaling.

In Fig. 8, we demonstrate how nonlinear absorption K_{NL} of the HYAS-BDF behaves at scaling excitation power (with emission maximum at ~2.07 μm) into its absorption band, peaking at almost the same wavelength (this band, refer to Fig. 2(a), is repeated in inset to Fig. 8 but at linear scaling). As was done at excitation into the NIR band of Bi(Al) BACS (refer to Fig. 6 and to the note therein), lengths of the fiber (<20 cm) were chosen to be relevant for clear fixation of the bleaching effect at around 2 μm (given its high absorption in

Optical Materials EXPRESS

this spectral domain). Note that the horizontal dashed arrow in Fig. 8 again marks the plateau, to which residual absorption approaches under the action of pump-light.

As seen from the figure, ~2-μm absorption is bleached quite effectively: at increasing P_{in} absorption is reduced to a level much lower (~5 dB/m) than its 'initial' (small-signal) value (~35 dB/m, as asterisked in the figure). The characteristic power that bleaches absorption, is low (~0.5 mW), being comparable with powers bleaching the ~1-μm band of the fiber: refer to Fig. 6. Note that the found effect of ~2-μm absorption bleaching in the HYAS-BDF may make fiber of this type employable as saturable absorber for Holmium doped fiber lasers.

Resuming, it is natural to propose that the presence of ~2.1-μm absorption band itself (never reported for Hf-free AS BDFs) and its easy bleaching at low-power 'in-band' excitation (Fig. 8) in the HYAS-BDF is inherent to the presence of some phototropic 'active' centers, formed due to co-doping with Bi and Hf/Y. Herein, we tentatively assign BACs of this kind as Bi(Hf). It also deserves mentioning that we did not register features like those presented by Fig. 8 in other AS based but Hf-free BDFs (in Fig. 9 below, such fibers are compared in terms of linear absorption spectra), which is in favor of our hypothesis that Bi(Hf) BACs are inherent to co-doping with Hf. On the other hand, in recently published paper [41], where authors report a saturable absorber based on germanosilicate BDF (for 1.93-μm), there is an absorption spectrum of this fiber in mid-IR, where a small peak at ~2.05…2.1 μm is clearly seen. It cannot be excluded that its origin is likely to what is observed in our HYAS-BDF due to co-doping with Hf, i.e. formation of some centers, active in mid-IR, but in [41] related to Ge co-doping.

Furthermore, it is worth of proposing that centers Bi(Hf) may fluoresce beyond 2.1 μm. Note that some indications of weak emission from the HYAS-BDF beyond ~2.1 μm were revealed from our experiments at ~2.07-μm broadband excitation, but indirectly (a positive signal resulted after making subtraction of input spectra from output ones). However, the latter issue requires an unambiguous and careful check in further experiments: it was too weak (if presented at all) for being reliably accessible with the currently available spectral equipment.

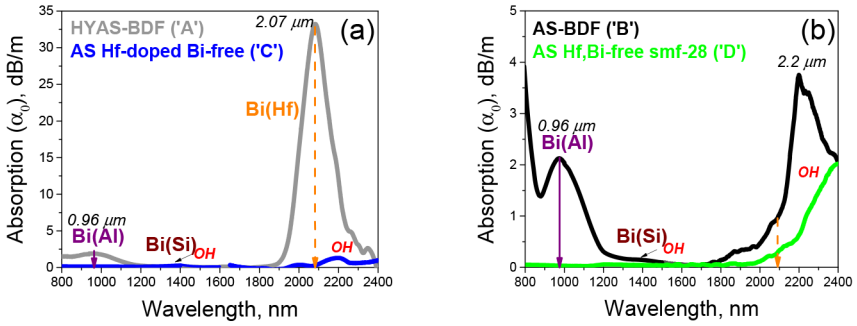

Fig. 9. Absorption spectra of (a) HYAS-BDF ('A') (grey curve) and AS Hf-doped Bi-free fiber ('C') (blue curve) and (b) AS Hf-free BDF ('B') (black curve) and AS Hf,Bi-free smf-28 '(D') (green curve). The spectra were obtained using OSA1/OSA2. The BACs associated with Al, Si, and Hf/Y are abbreviated as Bi(Al), Bi(Si), and Bi(Hf), respectively. The loss features at ~1.4/~2.2 μm (marked 'OH') are associated with OH^- groups contaminating.

Let's finally compare small-signal absorption spectra of AS fibers of a few types: see Fig. 9. In this figure, such spectra are shown for ('A') the HYAS-BDF; ('B') the AS (Hf-free) BDF; ('C') the AS co-doped with Hf (and Y) but Bi-free fiber, and ('D') the commercial AS (un-doped smf-28) fiber. As seen, absorption at ~2.0…2.1 μm is present in HYAS-BDF 'A' only, whereas in AS BDF 'B' it is absent, whereas strong loss of OH^- groups (peaking at ~2.2 μm) dominates in the region. Furthermore, in fiber 'C', co-doped with Hf but Bi-free, in contrast to HYAS-BDF 'A', there are no steps of loss at 2.0…2.1 μm. Thus, the intensive

Optical Materials EXPRESS

absorption peak at ~2.0…2.1 μm in the HYAS-BDF is undoubtedly related to co-doping with Bi and Hf/Y.

The other point to mention is that both Hf co-doped fibers ('A' and 'C') (a) demonstrate less in magnitude overall loss beyond 2 μm than the ones free from Hf doping ('B' and 'D') (b). This is another advantage of Hf-doping: fibers of HYAS type demonstrate significant reduction of 'fundamental' loss in mid-IR, as stated in [38] on the example of multimode HYAS-based fibers.

4. Conclusions

In this work, we report a spectral analysis of novel hafnia-yttria-alumina-silica (HYAS) based fiber doped with Bismuth (Bi). As shown, this fiber demonstrates in the NIR region all optical properties that stem from the presence of Bi-related active centers (BACs), associated with Al, viz. Bi(Al). This concerns a set of impactable characteristics: absorption and fluorescence spectra, fluorescence decay, resonant-absorption bleaching, fluorescence lifetime and gain, all inherent to BACs of this type. Notably, these properties of the fiber are inspected at laser-diode pumping at different wavelengths (at 908, 976, 1069, and 1120 nm), falling all into the NIR band of Bi(Al) BACs, thus permitting direct comparison of the results and the fiber's overall characterization. The found spectral laws permit one to determine an optimal on pump wavelength fluorescence/gain capacities of the fiber and its 'quality' in terms of absorption bleaching (ratio of bleached and residual absorptions), impactful for NIR applications at diode pumping. Furthermore, the HYAS based Bi-doped fiber is shown to be of better general performance as compared with its Hf-free analogs; for instance, it demonstrates less pronounced concentration-related effects such as up-conversion and longer NIR fluorescence lifetime. Seemingly, this stems from a property of HfO_2 to modify the core-glass structure, facilitate the dispersion of Bi ions and, eventually, diminish the clustering phenomena. Besides, another potentially useful feature of the HYAS based Bi doped fiber deserves emphasis: it provides, even at moderate (units of mol.%) co-doping with Hf, low fundamental loss beyond 2 μm, diminished by a few times as compared with 'conventional' silica-based fibers. This advantage may make fibers of HYAS type attractive for mid-IR applications. Furthermore, Hf ions in the core-glass of AS-type affect not only the local structure of Bi(Al) BACs but, most probably, assist in formation of BACs of other type, 'active' in mid-IR. This is revealed by our results, demonstrating the presence in this fiber of an intensive resonant-absorption band centered at ~2.1 μm, effectively bleachable by low-power (a few mW) 'in-band' excitation. The spectral analysis proceeded with this fiber and its aluminosilicate analogs (free from Bi or Hf) reveals that this type of centers, optically-active (viz., bleachable) in ~2.0…2.2-μm range, is adherent to co-doping with Bi and Hf/Y. We tentatively name them Bi(Hf) BACs but their nature is yet unclear and requires a comprehensive study in future.

Funding

CONACyT (via Project 242221, Mexico); Ministry of Education and Science of the Russian Federation through the Increase Competitiveness Program of NUST "MISiS" (via Grant K3-2017-015); DST (Govt. of India); internal project '2 microns' (Centro de Investigaciones en Optica Leon, Mexico).